AIMS Materials Science, 9(5): 733–749.
DOI: 10.3934/matersci.2022045
Received: 05 July 2022
Revised: 23 August 2022
Accepted: 04 September 2022
Published: 29 September 2022

http://www.aimspress.com/journal/Materials

Research article

Mechanical properties and dry sliding wear behaviour of Al–Si–Mg alloy by equal channel angular pressing

Nur Farah Bazilah Wakhi Anuar[1,3], Mohd Shukor Salleh[2,*], Mohd Zaidi Omar[3] and Saifudin Hafiz Yahaya[2]

[1] Faculty of Mechanical and Manufacturing Engineering Technology, Universiti Teknikal Malaysia Melaka, Hang Tuah Jaya, Durian Tunggal Melaka, 76100 Melaka, Malaysia
[2] Faculty of Manufacturing Engineering, Universiti Teknikal Malaysia Melaka, Hang Tuah Jaya, Durian Tunggal Melaka, 76100 Melaka, Malaysia
[3] Faculty of Engineering and Built Environment, Universiti Kebangsaan Malaysia, UKM Bangi, 43600 Selangor, Malaysia

* **Correspondence:** Email: shukor@utem.edu.my; Tel: +606-2702601.

Abstract: This study investigated the microstructure, hardness, tensile and tribological behaviour of a cooling slope Al–Si–Mg alloy following ECAP and T6 heat treatment. The optical and scanning electron microscopes were applied to investigate the microstructure of the as-cast material and heat-treated ECAPed Al–Si–Mg alloy. The dry sliding wear test was tested with three different loads of 10 N, 50 N, and 100 N with constant sliding speed and sliding distance at 1.0 m/s and 9000 m, respectively, using the pin-on-disc tribometer. The hardness and tensile properties were evaluated through microhardness, UTS, and YS measurement for the as-cast Al–Si–Mg alloy, both heat-treated with and without ECAPed alloys. Moreover, wear rate and COF in the Al–Si–Mg alloy with different loads were analysed and linked with microstructural and strength behaviour after the ECAP process. Meanwhile, these analyses of results were correlated with the behaviour of the as-cast Al–Si–Mg aluminium alloy and heat-treated non-ECAPed alloy. Results demonstrated that a combination of ECAP processing and T6 heat treatment improves the mechanical behaviour, while the COF and wear rate are improved at a load of 100 N.

Keywords: aluminium alloys; equal channel angular pressing; microstructure; mechanical properties; dry sliding wear; worn surface

1. Introduction

Aluminium alloys have been used extensively in a variety of applications, i.e., aerospace, marine, and automotive industries, because of their outstanding specific properties, exceptional toughness, endurance performance, castability and resistance to corrosion [1–3]. Nowadays, attention towards strengthening the characteristics of Al–Si aluminium alloy has expanded significantly. Al–Si aluminium alloy has great casting capabilities, corrosion resistance, and an excellent strength-to-mass ratio, particularly when applied correctly [4]. These characteristics make Al–Si alloys excellent for application in the automotive and aerospace industries [5]. The key variables leading to these features of Al–Si alloy are the rich α-Al phase and eutectic silicon element particles. Nevertheless, the shape of needle-like Si particle plates diminishes the mechanical characteristics, specifically, the ductility of the alloy [6]. Furthermore, it indicates that the wear qualities of Al–Si alloys produced by traditional casting degenerate to ferrous materials. Casting defects such as porous products and inclusions are common in conventional Al–Si alloys, which can impair the mechanical qualities of materials [7]. For that reason, the alteration of these silicon and eutectic structural systems can substantially improve the mechanical and physical properties of the alloy. It is necessary to make some modifications to alloys to overcome the shortcomings in conventional casting. Recent research has shown that a reduction in the size of the Si particles improves the strengthening properties as well as their resistance to wear [8,9].

Various fabrication procedures are currently employed to create appropriate slugs with non-dendritic microstructure, which is critical for semi-solid metal (SSM) processing. It includes mechanical stirring, strain-induced melt activation (SIMA), spray casting, grain refinement and cooling slope method, recrystallization and partial melting (RAP) [10]. SSM processing has been the focus of substantial studies since its introduction in the early 1970s [11]. Compared to other SSM approaches, the cooling slope method offers simplicity with minimal equipment and operating costs [7]. The cooling slope method creates a non-dendritic structure by pouring molten metal into a mould with moderate heat through an inclined cooling plate [12,13]. Although cast Al–Si alloys are commonly used for SSM processing, their mechanical behaviour may be insufficient when specific requirements in strength, fatigue and wear are required for particular purposes in the automotive and aerospace industries. Therefore, with the growing field and application scale development, the method to further enhance the properties of alloys and the potential to expand the application fully is an unending scientific question faced in the study of metal structural materials.

In the last 10 years, Al–Si alloys with fine grain sizes have been developed through research on severe plastic deformation processes (SPD) and the potential to produce Al–Si alloys with the required strength [14]. Equal channel angular pressing (ECAP) is a beneficial SPD processing technique for attaining metals with significant metallurgical alteration and high dislocation density. ECAP produces a product with a high degree of homogeneity and a uniform fine-grained structure evenly dispersed in the finished product [15,16]. In contrast to existing SPD strengthening techniques, the ECAP process can tightly control the deformation mechanism and the number of deformations and generate a sheet structure with one layer without fracturing the material [17]. It creates true layer strain and refines the grain to less than 1 μm of grain size, while the specimens are deformed without any geometry adjustment. Various researchers have attempted the ECAP processing on Al–Si alloys in many instances throughout the prior few years and obtained initial achievements in enhancing their strengths, elasticity, and fracture toughness [18–21]. These studies revealed that ECAPed alloys have superior mechanical properties compared to coarse-grained base alloys. For example, Jiang et al. [22] studied the effect of the deformation ECAP process on annealed Al–Mg–Mn–Sc–Zr alloy. It was discovered

that a single ECAP pass causes an extremely high shearing strain concentration, and the hardness was increased compared with non-ECAP processing due to high dislocation density and high recrystallization fraction after ECAP processing. In addition, Harničárová et al. [23] revealed that the grain size of AlMgSi0.5 was refined and decreased from 28.9 μm in the as-received AlMgSi0.5 alloy to 4.63 μm after the fourth ECAP passes, which led to an increase in strength from 210 MPa to 304 MPa.

There is limited finding made on the wear and friction behaviour of aluminium alloys. Investigations into the significance of the ECAP technique on the tribological characteristics of aluminium alloy have revealed a distinct impact on wear behaviour [24–26]. El Aal [27] investigated the rate of wear for ECAP-processed Al6061 alloys and reported that mass loss and the increase in the number of passes decreased the friction coefficient of Al6061 alloys. An increase in hardness after ECAP processing remarkably impacts the wear mechanism and its alteration. Pérez et al. [28] also reported that the volume loss of AA5083 after the dry sliding wear test was significantly reduced, and wear resistance was enhanced after two ECAP passes. An increase in the number of ECAP passes enhances the wear resistance due to increment in microhardness and grain refinement. Moreover, treatment processes based on solutioning and ageing are crucial to obtaining the optimal mechanical behaviour in alloys [29]. As a result, many researchers have been intrigued by the utilization of SPD on aluminium alloys, particularly on precipitation hardening (heat treatment) [16,30–32]. It is commonly recognized that the temperature and duration of a heat treatment significantly influence modification in the characteristics and microstructure of a material according to its potential purposes [33]. Snopiński et al. [34] reported that the density of AlSi10Mg was increased by about 5.16%. The microhardness value for as-built AlSi10Mg was the highest with 135 HV, however, it decreased to 101 HV after the heat treatment process due to poor hardness inhomogeneity. Multiple dislocations were induced in the material during the ECAP pass, resulting in a slight increase in microhardness to 133 HV after heat treatment and two ECAP passes.

Despite recent research have demonstrated that refinement of aluminium alloys microstructure through the ECAP process results in improvement in the mechanical characteristics of the materials [14,15,18,35,36], there is a lack of research investigating the mechanical and tribological characteristics of cooling slope heat-treated ECAPed Al–Si alloy. Thus, the present study aimed to evaluate the significance and influence of ECAP processes on the hardness and tensile properties, as well as the wear behaviour of T6 heat-treated Al–Si–Mg alloy. In addition, microstructural alteration after ECAP leading to change in mechanical and wear properties was also examined. The results were compared with those without ECAP processes and as-cast material.

2. Materials and methods

2.1. Specimen preparation using cooling slope casting

Commercial Al–Si–Mg alloy with chemical composition, as shown in Table 1, was employed in this investigation. The spherical microstructure was obtained through the application of the cooling slope approach, as shown in Figure 1.

Table 1. Chemical composition of studied Al–Si–Mg aluminium alloy in wt.%.

Si	Mg	Fe	Cu	Mn	Zn	Ni	Pb	Sn	Ti	Cr	Ca	Al
7.56	0.22	0.46	0.05	0.19	0.01	0.01	0.01	0.01	0.04	0.01	0.01	Remainer

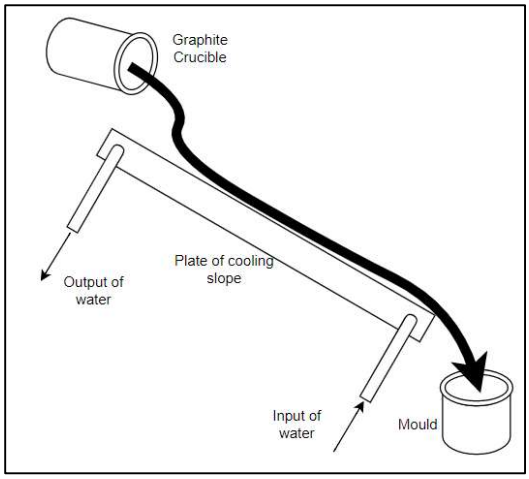

Figure 1. Schematic diagram of cooling slope casting apparatus used.

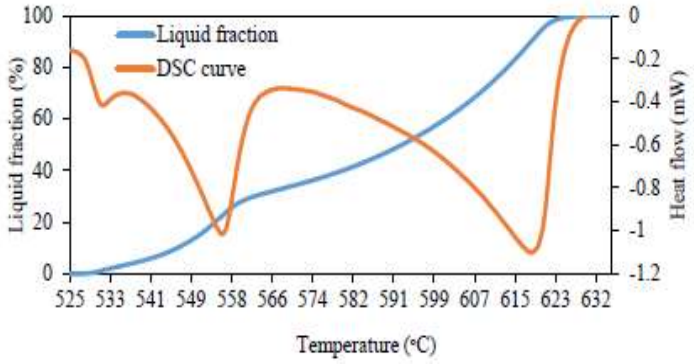

Figure 2. Liquid fraction versus temperature of Al–Si–Mg alloy.

The commercial ingot was heated in a graphite crucible until it melted at 700 ℃, and the molten state was maintained for 5 min to ensure that the alloy had completely melted. The molten temperature was reduced to the required pouring temperature of 625 ℃ and the molten was poured onto the cooling slope plate. The plate of the cooling slope was adjusted to a length of 300 mm at a 60° inclination angle with a circulation of coolant water at the bottom of the plate to enhance the nucleation rate of the α-Al solid phase. The boron nitride (BN) was applied to coat the surface of the cooling slope to prevent adhesion between molten metal and the surface of the plate. Next, molten metal was poured into a cylindrical mild steel mould preheated at 150 ℃ to form 120 mm in height and 25 mm in diameter feedstock and cooled to room temperature. The melting temperatures for pouring were chosen to minimize the melt superheat based on differential scanning calorimetry (DSC) analytical as-cast data, as shown in Figure 2. A few feedstock samples were formed by pouring the molten Al–Si–Mg alloy at 700 ℃ without using the cooling slope method in the preheated mould to compare the influence of

equal channel angular pressing (ECAP) with conventional casting.

2.2. ECAP processing

The feedstocks of the as-cast alloy and cooling slope cast Al–Si–Mg alloy were machined into a cylindrical billet with a length of 80 mm and a diameter of 15 mm. The billets were subjected to annealing at 540 ℃ for 8 h in a Nabertherm Controller B180 furnace and left until it cooled down at room temperature. All the annealed billets were subjected to ECAP processing up to two passes using route A without involving any rotation. The ECAP processing was performed with 0.1 mm/s pressing velocities at room temperature. Molybdenum disulphide (MoS_2) lubricant was applied to decrease the resistance between the die and billets to improve the surface finishing of the samples and reduce the ECAP load. A die with a channel angle of 120° with a circular cross-section and a curvature angle of 30° was employed. In this study, the friction factor was disregarded due to the use of the lubricant. The ECAPed billet samples (as-cast and cooling slope) were subjected to the T6 heat treatment, where solution treatment was maintained at 540 °C for 8 h, quenched by room temperature water, and aged at 155 ℃ for 3 h.

2.3. Microstructure characterization

All ECAPed samples were cut from the billets for microstructure evaluation. All samples were ground with grinding silicon carbide abrasive paper (grit 240–1200 fine), followed by polishing with 3 μm and 1 μm of diamond pastes, respectively. These samples were etched with Keller's reagent solution (95 mL of distilled water, 2.5 mL of nitric acid, 1.5 mL of hydrochloric acid and 1 mL of hydrofluoric acid) for 7 s. The microstructure of heat-treated ECAPed samples for conventional as-cast and the cooling slope was evaluated by an optical microscope (Olympus optical microscope). Characterization of various phases of polished and etched samples was carried out using Carl Zeiss scanning electron microscope (SEM) and X-ray diffraction (XRD).

2.4. Mechanical testing

The heat-treated ECAPed samples for as-cast and cooling slopes were subjected to microhardness and tensile tests. The microhardness test was carried out using Mitutoyo micro Vickers tester under a load of 1000 gf with an indentation time of 5 s. Each sample was measured at least 10 times. All samples for the microhardness test were ground with silicon carbide abrasive paper and polished to avoid inaccurate hardness values. The tensile specimens were cut parallel to the pressing direction and machined according to the ASTM E8 standard (diameter of 2.5 mm and a gauge length of 10 mm). The tensile test was performed using the Instron Universal Testing Machine (UTM). The test was conducted at a displacement rate of 1 mm/min and a load of 100 kN and was repeated three times to obtain the average strength value.

2.5. Dry sliding test

The as-cast and cooling slope samples of ECAPed were subjected to dry sliding wear testing with a DUCOM pin-on-disc type wear test machine, and the M2 tool steel disc (62 HRC with less than 0.3 μm of surface roughness) was used as counterface material. Dry sliding wear tests were

conducted using the applied load of 10 N, 50 N, and 100 N at room temperature, with a constant sliding distance of 9000 m and a constant sliding speed of 1.0 m/s. The surface of pin specimens for wear tests was ground using grinding papers (400, 600, 800 and 1200) and polished 3 μm and 1 μm diamond paste to obtain less than 0.2 μm surface roughness since the wear is influenced by surface roughness and flatness. All the specimen pins of the dry sliding wear test were cleaned with acetone in an ultrasonic cleaning machine and weighed before testing. Each loading was repeated three times. The difference in weight before and after the wear test was used to measure density using volumetric wear loss based on Archimedes' principle. Meanwhile, the coefficient of friction was recorded during the wear test, and the data were retrieved from a system to obtain the coefficient of friction through calculation. The wear mechanism was identified by observing the worn surfaces under a scanning electron microscope (SEM).

3. Results and discussions

3.1. Microstructure analysis

Figure 3a shows the optical microscope images of the as-cast Al–Si–Mg, while Figures 3b,c,d,e shows the microstructure after T6 heat treatment for as-cast Al–Si–Mg, cooling slope as-cast, cooling slope as-cast with one ECAP pass, and cooling slope as-cast with two ECAP passes, respectively. The microstructure of the as-cast Al–Si–Mg (Figure 3a) exhibits needle-like shaped eutectic silicon and transitions to refinement after ECAP with two passes (Figure 3e). The T6 heat treatment allows the dispersion of fine silicon particles and intermetallic compounds homogeneously. Furthermore, it was obvious that there was a significant difference in the microstructure of the cooling slope heat-treated ECAP deformation process alloy following the T6 heat treatment. Figure 4 and Figure 5 show the magnification image along with the identification elemental by X-ray spectrum (EDX) of one of the second phase particles for cooling slope heat-treated ECAPed sample alloy. It was discovered that after two ECAP passes process, the silicon particles were intensified within the globular α-Al while the other elementary particles, including copper, magnesium and iron, were homogeneously dispersed in all ECAPed alloys as identified in EDX in Figure 5. The ECAP deformation process increases the precipitation kinetics by providing a nucleation site to induce a dislocation [36]. The morphology of eutectic silicon particles after two ECAP passes was more spheroidal (Figure 5) than the one in Figure 4. The EDX analysis shows the existence of a few elements such as silicon (Si), copper (Cu), magnesium (Mg) and iron (Fe) elements clearly at the grain boundaries in the aluminium (Al) matrix, as shown in SEM and EDX patterns. The bright contrast phases identified by EDX in Figure 4 and Figure 5 marked at point B, respectively, are composed of aluminium, copper, magnesium, silicon and iron, which is recommended as the needle-like intermetallic phase.

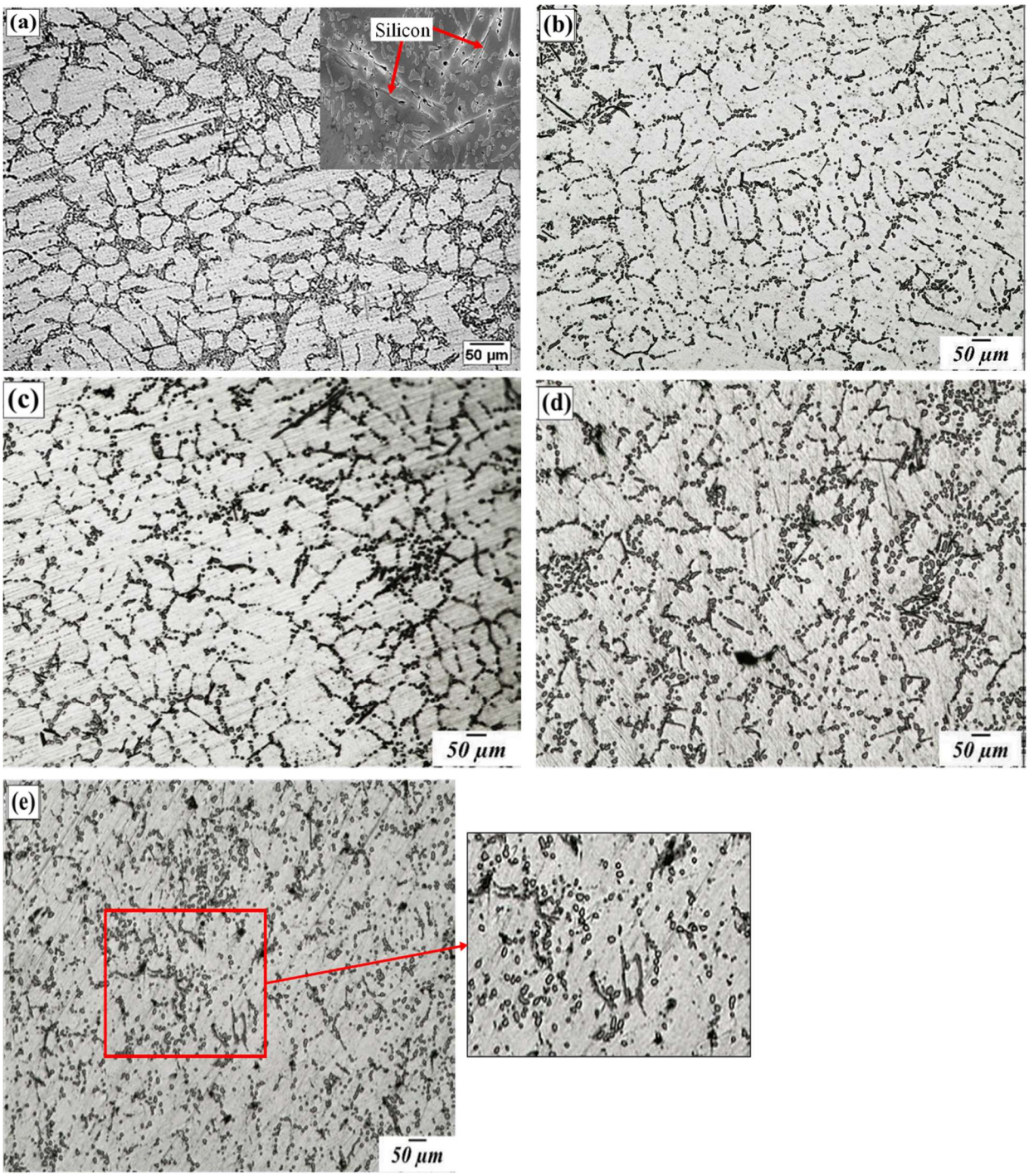

Figure 3. Optical illustration of (a) as-cast Al–Si–Mg, T6 heat treatment of (b) as-cast Al–Si–Mg, (c) cooling slope as-cast Al–Si–Mg, (d) cooling slope as-cast Al–Si–Mg with one ECAP pass, and (e) cooling slope as-cast Al–Si–Mg with two ECAP passes.

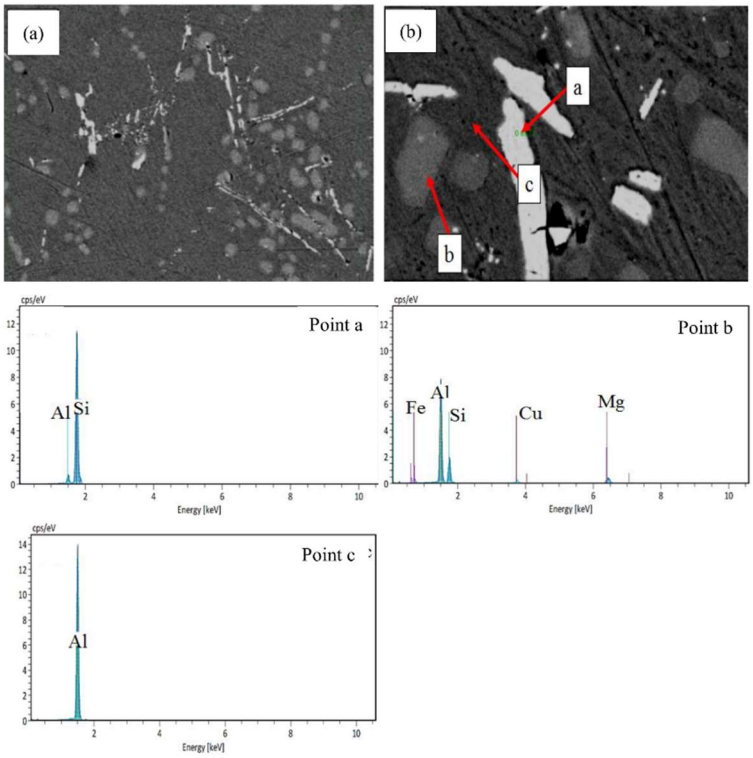

Figure 4. Microstructure of cooling slope heat-treated with one ECAP pass condition, (a) general aspect of microstructure by SEM, and (b) EDX spectrum of phase particles in the microstructure.

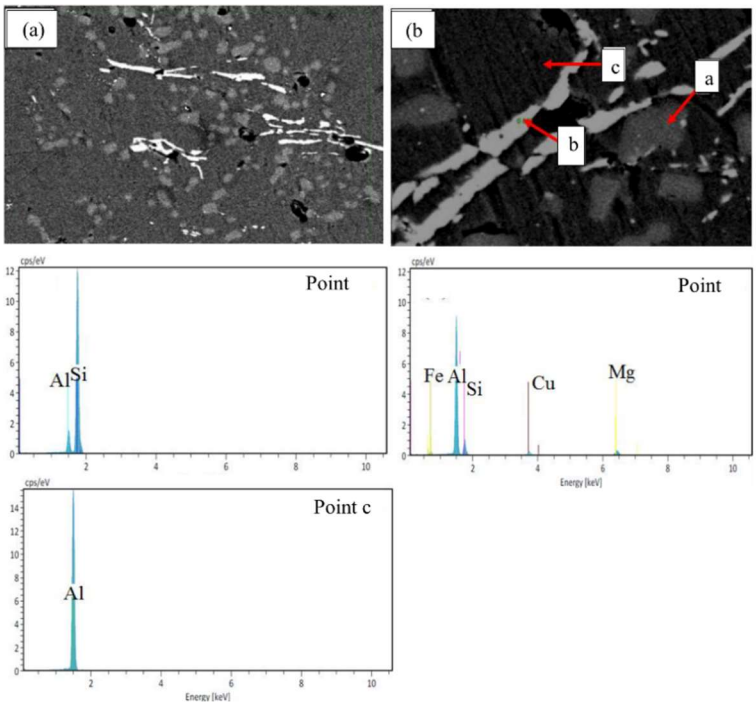

Figure 5. Microstructure of cooling slope heat-treated with two ECAP passes conditions, (a) general aspect of microstructure by SEM, and (b) EDX spectrum of phase particles in the microstructure.

3.2. Hardness and tensile properties

Hardness and tensile properties of cooling slope as-cast and cooling slope with ECAPed treated with T6 heat treatment are presented in Figure 6 and Figure 7, respectively. Figure 6 shows that the hardness of the alloy with two ECAP passes treated with T6 heat treatment is greater than that of the heat-treated as-cast alloy and heat-treated alloy with one ECAP pass. Figure 7 illustrates that the tensile strength of heat-treated ECAPed alloy is also enhanced with the increase of ECAP pass number compared to the heat-treated non-ECAPed alloy. The enhanced hardness of the heat-treated ECAPed alloy is due to the decrease in the grain size of the α-Al primary phase, as well as the homogeneous distribution of the intermetallic phase and the reduction of microporosity obtained in the sample as the number of ECAPed passes increases. The T6 heat treatment process allows some of the alloying elements to melt back into the α-Al phase matrix at high temperature and solid solution strengthening. In addition, the ageing process allows the shallow α-Al solvus curve to create a greater quantity of precipitating phases and provide alloying components with lower solids to dissolve in aluminium at a certain ageing temperature [37]. This is due to the presence of intermetallic phases, which create a restriction to dislocation movement and demonstrate a higher resistance to deformation. In addition, the transition effects of heat-treated ECAP and non-ECAP on elongation are shown in Figure 7, which reports the reduction in elongation of heat-treated alloys with two passes of ECAP and one pass of ECAP by 50.16% and 30.65% compared to as-cast Al–Si–Mg alloy, respectively. The improvement in tensile elongation before fracture is associated with the alteration in the shape of eutectic silicon particles in the Al–Si–Mg alloy and grain refinement. However, the tensile elongation of heat-treated non-ECAPed alloys is higher compared to as-cast Al–Si–Mg. This behaviour may be attributed to the decrease in dislocation density after the T6 heat treatment process, which generates another space zone for the fourth deformation and deferred fracture and necking. The presence of pores in the materials during cooling slope without deformation facilitates the growth of microcracks and decreases the effectiveness of the material, which also results in the increment in the elongation of non-ECAPed alloys. Thus, an increase in both hardness and tensile, as well as the reduction in elongation by ECAP and heat treatment process as a response to the re-distribution of precipitates, can be attributed to high dislocation density and grain refinement of microstructure [14]. Heat-treated ECAPed Al–Si–Mg alloys have minimal porosity due to deformation, and it was discovered that the small and fined spherical α-Al phase increases the mechanical and strength behaviour of the aluminium alloy [11,38]. Therefore, the improvement in mechanical characteristics reported in heat-treated ECAPed Al–Si–Mg alloy is primarily due to the phase transition and combination impact of the particular structure adjustments in the size and shape of silicon. The intermetallic particles were also identified as a result of work-hardening during the ECAP process, which reduced the porosity level and grain diameter of the α-Al primary grain compared to the Al–Si–Mg alloy without ECAP.

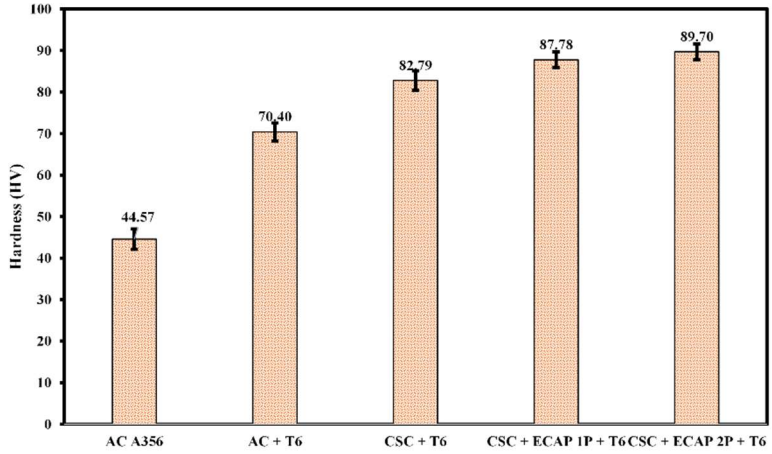

Figure 6. The hardness properties of heat-treated ECAPed Al–Si–Mg alloy and non-ECAPed Al–Si–Mg alloy. The ECAP process accelerates the precipitation kinetics and increases hardness due to induced strain.

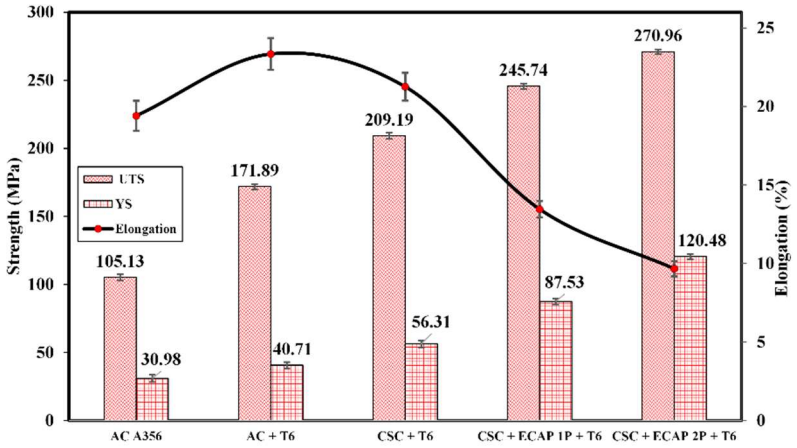

Figure 7. Ultimate tensile strength (UTS), yield strength (YS), and elongation of as-cast Al–Si–Mg alloy, heat-treated as-cast Al–Si–Mg, cooling slope heat-treated non-ECAPed alloys and cooling slope heat-treated ECAPed alloys, respectively.

3.3. Wear analysis

The influence of ECAP and T6 heat treatment on the samples worn through a dry sliding wear test with three different applied loads of 10 N, 50 N, and 100 N, a constant sliding distance of 9000 m and a constant 1.0 m/s sliding speed, is shown in Figure 8. The figure demonstrates the slightly lower wear rate of the cast formed by cooling slope and heat treatment with two ECAP passes than that of other cast alloy formed via cooling slopes heat treatment only. At a normal load of 10 N, the wear rate of the as-cast Al–Si–Mg alloy was 6.99×10^{-5} mm^3/N.m and 5.52×10^{-5} mm^3/N.m for Al–Si–Mg formed by cooling slope and heat treatment, which is distinct with 3.87×10^{-5} mm^3/N.m and 3.36×10^{-5} mm^3/N.m for alloys formed by cooling slope and heat treatment with one and two ECAP passes, respectively. The rate of wear decreased with an increase in normal load for both non-ECAPed and ECAPed alloys. However, the wear rate was increased for heat-treated as-cast and alloy

from cooling slope at a load of 50 N compared to heat-treated ECAPed alloy, which can be described using microstructural characteristics as shown in Figures 3b,c,e. Such differences are due to the feasibility of microstructural characteristics such as shape, size, dispersion of strong intermetallic phases and dispersion particles of Si in the T6 heat treatment process that have a significant impact on dry sliding wear achievement [11,39,40]. This could be attributed to the affiliation of cooling slope casting and T6 heat treatment without ECAP processing, which results in a significantly less uniform dispersion of silicon particles. In addition, the ECAP technique has been claimed to improve wear resistance with enhanced hardness for various alloys in recent years [14,17,24]. According to Alhawari et al. [12] and Thuong et al. [11], higher loads promote strain hardening of contact materials. The increase in load leads to an increase in frictional force, which increases deformation and impedes the movement of dislocations, resulting in strain hardening of the material. As a result, the abrasion resistance increases, which eventually leads to an improvement in wear resistance. In addition, a larger surface area in contact with the surface of the disc counter promotes asperities. Thus, this gripping action contributes to a slower wear rate of the samples when heavier loads are applied. The relation between the coefficient of friction and the applied load of 10 N, 50 N, and 100 N at a sliding distance of 9000 m and 1.0 m/s sliding speed for both alloys formed by cooling slope and heat treatment with and without ECAP are illustrated in Figure 9. The average coefficient of friction for all samples decreased with the increasing load, of which the value for alloy formed by cooling slope and heat treatment with two ECAP passes is lower than that of other samples. Mechanical qualities such as hardness and shear strength influence the wear rate and coefficient of friction. The decrease in friction coefficient as the hardness increases is due to the grain refining. In addition, T6 heat treatment has also increased the microhardness of the Al–Si–Mg alloy, resulting in increased strength and decreased average friction coefficient of ECAPed Al–Si–Mg alloy compared to that of as-cast and non-ECAPed alloy.

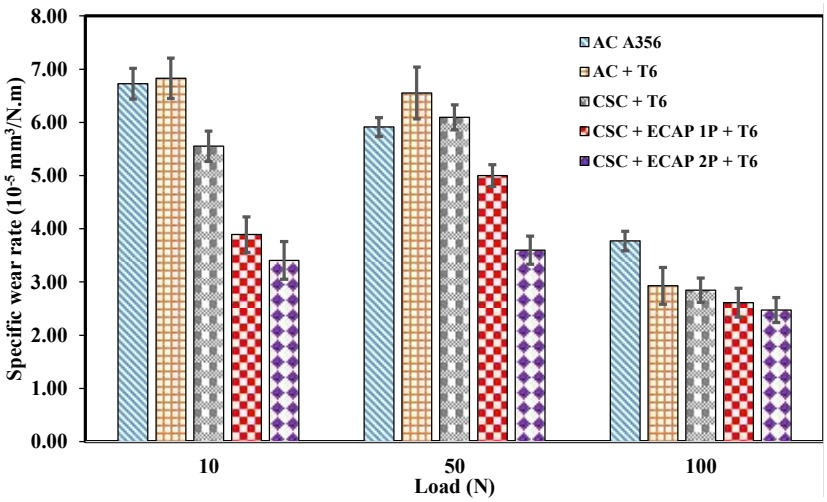

Figure 8. The variations of wear rate versus normal load for as-cast Al–Si–Mg alloy, heat-treated as-cast Al–Si–Mg, cooling slope untreated ECAPed alloys and cooling slope heat-treated ECAPed alloys.

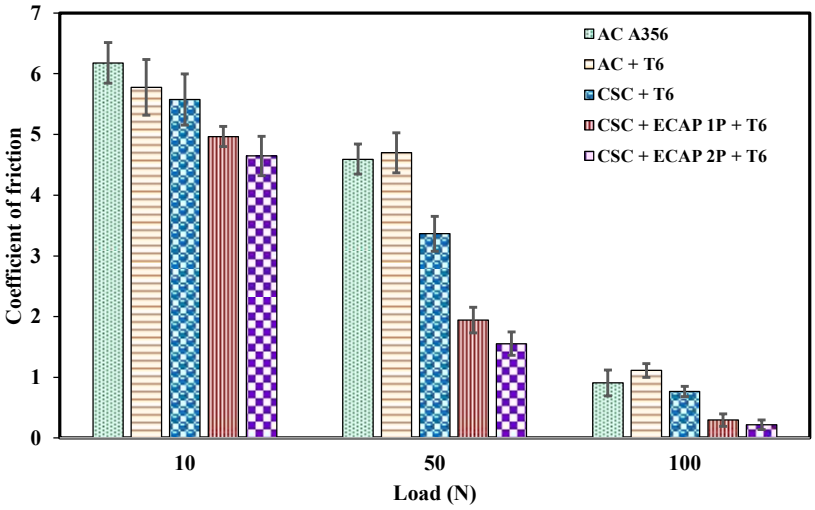

Figure 9. The variations in the coefficient of friction versus normal load for as-cast Al–Si–Mg alloy, heat-treated as-cast Al–Si–Mg, cooling slope untreated ECAPed alloys and cooling slope heat-treated ECAPed alloys.

Illustrations of wear mechanisms of the samples produced by cooling slope and heat treatment with and without ECAP processing, i.e., the wear mechanism under SEM, are shown in Figure 10. The worn surface of non-ECAPed is characterized by wide and deep grooves with small craters subjected to the high stress of 100 N. The figure demonstrates that the worn surface of the as-cast Al–Si–Mg alloy and the heat-treated non-ECAPed alloy are more ravaged than of ECAP-T6 samples. On the contrary, the ECAPed alloy exhibits less grooves and shallow craters under the same conditions. Based on SEM images, the depth and breadth of the continual grooves in heat-treated as-cast samples (Figure 10b) are greater than that of heat-treated ECAPed samples (Figures 10d,e). Hard particles create deep grooves on the worn surfaces, which scrape the exterior surfaces of the specimen on its entrapment. The shear activity on Al creates deformation particles, and as a result, strong particles are derived from the separation of the second phase from the shear activity. This also demonstrates that craters generated on the worn track as a result of a high-stress abrasion on the coarsely equiaxed or flake-like shape, such as the needle-like intermetallic or element phase, have a negative impact on the wear resistance [7]. Thus, particles are weakly attached to the matrix, and the interfaces between the phase and the matrix are susceptible to microcracking. The worn surfaces of heat-treated alloy with two passes of ECAP at a high load of 100 N demonstrated a highly smooth and adherent marking, suggesting sample flow. Due to the applied load, considerable plastic deformation where the dislocation of motion is allowed to slip on the outer surface layer of the material induces heating of the worn surface, creating ductility in the alloy. As a result, adhesive wear develops in the heat-treated sample with two passes of ECAP. Therefore, it can be concluded that abrasive, and delamination wears are the main wear mechanism for the as-cast Al–Si–Mg and heat-treated as-cast without ECAP, while adhesive wear is the main wear mechanism for heat-treated after ECAP with two passes.

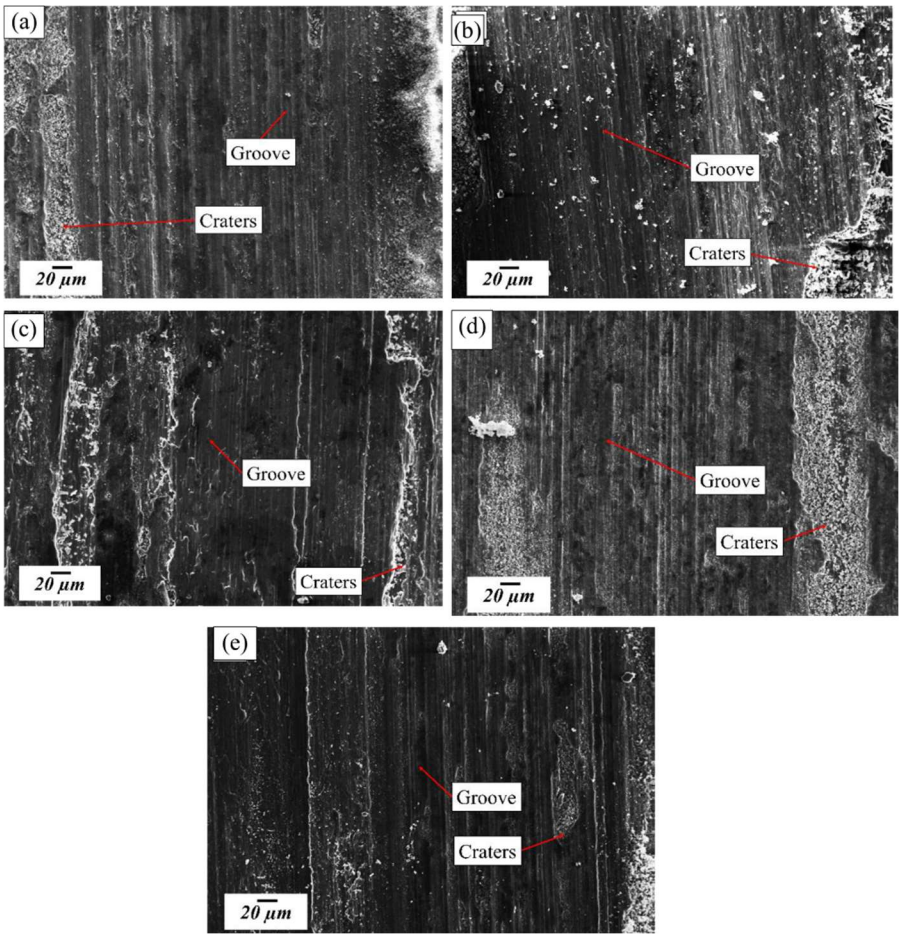

Figure 10. SEM images of the worn surface at 100 N applied load for (a) as-cast Al–Si–Mg, (b) as-cast heat-treated Al–Si–Mg, (c) cooling slope heat-treated Al–Si–Mg, cooling slope heat-treated for (d) one of ECAP pass and (e) two ECAP passes, respectively.

4. Conclusions

The equal-channel angular pressing (ECAP) processing and T6 heat treatment were applied to the as-cast Al–Si–Mg alloy to improve its microstructure, mechanical properties and wear behaviors. The main findings and conclusions of this study can be summarized as follows:

1. As-cast Al–Si–Mg alloy was successfully processed by T6 heat treatment and ECAP up to two passes following route A at room temperature.

2. ECAP processing assists the disintegration of needle-shaped silicon particles into a more uniform distribution than non-ECAPed alloys. In addition, the primary α-Al phase was refined after two passes of ECAP.

3. T6 heat treatment greatly influences the spheroidal of eutectic silicon particles for ECAPed Al–Si–Mg alloys compared to as-cast Al–Si–Mg alloy.

4. Two ECAP passes with T6 heat treatment significantly increased the hardness at 89.7 HV compared to the as-cast Al–Si–Mg alloy at 44.6 HV, while the tensile strength improved at 120.48 MPa compared to the as-cast Al–Si–Mg alloy at 30.98 MPa. The enhancement in the strength of both alloys is attributable to the highly uniform distribution and refinement of primary α-Al phase and Si particles in the cooling slope heat-treated ECAPed alloy.

5. The wear rate and the friction coefficient of heat-treated Al–Si–Mg alloy with ECAP processing were found lower than that of as-cast Al–Si–Mg alloy at the load of 10 N, 50 N and 100 N. The finding suggests that the enhancement in hardness and tensile strength, uniform distribution and finer grain of Si particles, and intermetallic phases are responsible for the increase in wear resistance. As the real contact surface increases, the increased gripping action between the pin and disc counter surfaces causes the wear rate to decrease when the normal load increases.

6. The wear mechanism shifted from abrasive and delamination wear for as-cast Al–Si–Mg and heat-treated as-cast without ECAP samples into adhesive wear for heat-treated alloys with two passes of ECAP.

Acknowledgements

The authors would like to thank Universiti Teknikal Malaysia Melaka (UTeM), Universiti Kebangsaan Malaysia and the financial support received under research grant PJP/2021/FKP/S01812.

Conflict of interest

The authors declare no conflict of interest.

References

1. Awotunde MA, Adegbenjo AO, Obadele BA, et al. (2019) Influence of sintering methods on the mechanical properties of aluminium nanocomposites reinforced with carbonaceous compounds: A review. *J Mater Res Technol* 8: 2432–2449. https://doi.org/10.1016/j.jallcom.2021.163321
2. Ali AM, Omar MZ, Hashim H, et al. (2021) Recent development in graphene-reinforced aluminium matrix composite: A review. *Rev Adv Mater Sci* 60: 801–817. https://doi.org/10.1515/rams-2021-0062
3. Abbasipour B, Niroumand B, Vaghefi SMM, et al. (2019) Tribological behavior of A356−CNT nanocomposites fabricated by various casting techniques. *T Nonferr Metal Soc* 29: 1993–2004. https://doi.org/10.1016/S1003-6326(19)65107-1
4. Zhuo X, Zhang Q, Liu H, et al. (2022) Enhanced tensile strength and ductility of an Al–6Si–3Cu alloy processed by room temperature rolling. *J Alloys Compd* 899: 163321. https://doi.org/10.1016/j.jallcom.2021.163321
5. Öztürk İ, Ağaoğlu GH, Erzi E, et al. (2018) Effects of strontium addition on the microstructure and corrosion behavior of A356 aluminum alloy. *J Alloys Compd* 763: 384–391. https://doi.org/10.1016/j.jallcom.2018.05.341
6. Wu Y, Liu C, Liao H, et al. (2021) Joint effect of micro-sized Si particles and nano-sized dispersoids on the flow behavior and dynamic recrystallization of near-eutectic Al–Si based alloys during hot compression. *J Alloys Compd* 856: 158072. https://doi: 10.1016/j.jallcom.2020.158072.
7. Abdelgnei MA, Omar MZ, Ghazali MJ, et al. (2020) Dry sliding wear behaviour of thixoformed Al–5.7Si–2Cu–0.3Mg alloys at high temperatures using Taguchi method. *Wear* 442: 203134. https://doi.org/10.1016/j.wear.2019.203134
8. Liu S, Zhang X, Peng HL, et al. (2020) In situ nanocrystals manipulate solidification behavior and microstructures of hypereutectic Al–Si alloys by Zr-based amorphous alloys. *J Mater Res Technol* 9: 4644–4654. https://doi.org/10.1016/j.jmrt.2020.02.091

9. Rahman AA, Salleh MS, Othman IS, et al. (2020) Investigation of mechanical & wear characteristics of T6 heat treated thixoformed aluminium alloy composite. *J Adv Manuf Technol* 14: 1–14.
10. Li N, Mao W, Geng X (2022) Preparation of semi-solid 6061 aluminum alloy slurry by serpentine channel pouring. *Trans Nonferrous Met Soc China* 32: 739–749. https://doi.org/10.1016/S1003-6326(22)65829-1
11. Van Thuong N, Zuhailawati H, Seman AA, et al. (2015) Microstructural evolution and wear characteristics of equal channel angular pressing processed semi-solid-cast hypoeutectic aluminum alloys. *Mater Des* 67: 448–456. https://doi.org/10.1016/j.matdes.2014.11.054
12. Alhawari KS, Omar MZ, Ghazali MJ, et al. (2015) Evaluation of the microstructure and dry sliding wear behaviour of thixoformed A319 aluminium alloy. *Mater Des* 76: 169–180. https://doi.org/10.1016/j.matdes.2015.03.057
13. Hanizam H, Salleh MS, Omar MZ, et al. (2020) Effects of hybrid processing on microstructural and mechanical properties of thixoformed aluminum matrix composite. *J Alloys Compd* 836: 155378. https://doi.org/10.1016/j.jallcom.2020.155378
14. Palacios-Robledo D, Fresneda-García J, Lorenzo-Bonet E, et al. (2021) Tribological analysis in Al–Mg–Zn alloy casting processed through equal channel angular pressing, compared with Al–7075 T6 alloy. *Wear* 476: 203680. https://doi.org/10.1016/j.wear.2021.203680
15. Jiang F, Tang L, Huang J, et al. (2019) Influence of equal channel angular pressing on the evolution of microstructures, aging behavior and mechanical properties of as-quenched Al–6.6Zn–1.25Mg alloy. *Mater Charact* 153: 1–13. https://doi.org/10.1016/j.matchar.2019.04.031
16. Baghbani Barenji A, Eivani AR, Hasheminiasari M, et al. (2020) Effects of hot forming cold die quenching and inter-pass solution treatment on the evolution of microstructure and mechanical properties of AA2024 aluminum alloy after equal channel angular pressing. *J Mater Res Technol* 9: 1683–1697. https://doi.org/10.1016/j.jmrt.2019.11.092
17. Liu M, Chen J, Lin Y, et al. (2020) Microstructure, mechanical properties and wear resistance of an Al–Mg–Si alloy produced by equal channel angular pressing. *Prog Nat Sci Mater Int* 30: 485–493. https://doi.org/10.1016/j.pnsc.2020.07.005
18. Dan S, Guowei W, Zhikai Z, et al. (2020) Developing a high-strength Al–11Si alloy with improved ductility by combining ECAP and cryorolling. *Mater Sci Eng A* 773: 138880. https://doi.org/10.1016/j.msea.2019.138880
19. Damavandi E, Nourouzi S, Rabiee SM, et al. (2019) Effect of ECAP on microstructure and tensile properties of A390 aluminum alloy. *Trans Nonferrous Met Soc China* 29: 931–940. https://doi.org/10.1016/S1003-6326(19)65002-8
20. Natori K, Utsunomiya H, Tanaka T (2021) Forming of thin-walled cylindrical cup by impact backward extrusion of Al–Si alloys processed by semi-solid cast and ECAP. *J Mater Process Technol* 297: 117277. https://doi.org/10.1016/j.jmatprotec.2021.117277
21. Bochvar NR, Rybalchenko OV, Tabachkova NY, et al. (2021) Kinetics of phase precipitation in Al–Mg–Si alloys subjected to equal-channel angular pressing during subsequent heating. *J Alloys Compd* 881: 160583. https://doi.org/10.1016/j.jallcom.2021.160583
22. Jiang J, Jiang F, Zhang M, et al. (2021) The recrystallization behavior of shear band in room temperature ECAPed Al–Mg–Mn–Sc–Zr alloy. *Mater Charact* 175: 111081. https://doi.org/10.1016/j.matchar.2021.111081

23. Harničárová M, Valíček J, Kušnerová M, et al. (2022) Structural and mechanical changes of AlMgSi0.5 Alloy during extrusion by ECAP method. *Materials* 15: 2020. https://doi.org/10.3390/ma15062020
24. Avcu E (2017) The influences of ECAP on the dry sliding wear behaviour of AA7075 aluminium alloy. *Tribol Int* 110: 173–184. https://doi.org/10.1016/j.triboint.2017.02.023
25. Ramu P, Reddy RHK, Kumar BK, et al. (2021) Investigation of wear characteristics of Al6061-Si_3N_4composites subjected to strain hardening through equal channel angular pressing. *Mater Today Proc* 46: 790–794. https://doi.org/10.1016/j.matpr.2020.12.765
26. Sureshkumar P, Jagadeesha T, Natrayan L, et al. (2022) Electrochemical corrosion and tribological behaviour of AA6063/Si_3N_4/$Cu(NO_3)_2$ composite processed using single-pass $ECAP_A$ route with 120° die angle. *J Mater Res Technol* 16: 715–733. https://doi.org/10.1016/j.jmrt.2021.12.020
27. Abd El Aal MI (2020) The influence of ECAP and HPT processing on the microstructure evolution, mechanical properties and tribology characteristics of an Al6061 alloy. *J Mater Res Technol* 9: 12525–12546. https://doi.org/10.1016/j.jmrt.2020.08.099
28. Luis Pérez CJ, Luri Irigoyen R, Fuertes Bonel JP, et al. (2020) Experimental and FEM analysis of wear behaviour in AA5083 ultrafine-grained cams. *Metals* 10: 479. https://doi.org/10.3390/met10040479
29. Al-Furjan MSH, Hajmohammad MH, Shen X, et al. (2021) Evaluation of tensile strength and elastic modulus of 7075-T6 aluminum alloy by adding SiC reinforcing particles using vortex casting method. *J Alloys Compd* 886: 161261. https://doi.org/10.1016/j.jallcom.2021.161261
30. Rominiyi AL, Oluwasegun KM, Olawale JO, et al. (2021) Effect of post-ECAP aging on the microstructure, hardness and impact behaviour of 6061 Al alloy. *Mater Today Proc* 38: 1031–1034. https://doi.org/10.1016/j.matpr.2020.05.670
31. Elhefnawey M, Shuai GL, Li Z, et al. (2021) On achieving ultra-high strength and improved wear resistance in Al–Zn–Mg alloy via ECAP. *Tribol Int* 163: 107188. https://doi.org/10.1016/j.triboint.2021.107188
32. Hu Y, Zhang Y, Zeng Q, et al. (2021) Achieving nanoscale Al_2Cu dispersoids in wrought Al-4.5wt.%Cu alloy by semi-solid isothermal treatment and post room-temperature ECAP. *Mater Lett* 305: 130787. https://doi.org/10.1016/j.matlet.2021.130787
33. Chak V, Chattopadhyay H (2020) Fabrication and heat treatment of graphene nanoplatelets reinforced aluminium nanocomposites. *Mater Sci Eng A* 791: 139657. https://doi.org/10.1016/j.msea.2020.139657
34. Snopiński P, Woźniak A, Pagáč M (2021) Microstructural evolution, hardness, and strengthening mechanisms in SLM AlSi10Mg alloy subjected to Equal-Channel Angular Pressing (ECAP). *Materials* 14: 7598. https://doi.org/10.3390/ma14247598
35. Zhao Y, Liu J, Topping TD, et al. (2021) Precipitation and aging phenomena in an ultrafine grained Al–Zn alloy by severe plastic deformation. *J Alloys Compd* 851: 156931. https://doi.org/10.1016/j.jallcom.2020.156931
36. Rymer LM, Winter L, Hockauf K, et al. (2021) Artificial aging time influencing the crack propagation behavior of the aluminum alloy 6060 processed by equal channel angular pressing. *Mater Sci Eng A* 811: 141039. https://doi.org/10.1016/j.msea.2021.141039
37. Nithesh K, Gowrishankar MC, Nayak R, et al. (2021) Effect of light weight reinforcement and heat treatment process parameters on morphological and wear aspects of hypoeutectic Al–Si based composites–a critical review. *J Mater Res Technol* 15: 4272–4292. https://doi.org/10.1016/j.jmrt.2021.10.019

38. Alhawari KS, Omar MZ, Ghazali MJ, et al. (2017) Microstructural evolution during semisolid processing of Al–Si–Cu alloy with different Mg contents. *Trans Nonferrous Met Soc China* 27: 1483–1497. https://doi.org/10.1016/S1003-6326(17)60169-9
39. Li Y, Yang M, Li M, et al.(2021) In-situ study of effects of heat treatments and loading methods on fracture behaviors of a cast Al–Si alloy. *Mater Today Commun* 28: 102680. https://doi.org/10.1016/j.mtcomm.2021.102680
40. Liu G, Gao J, Che C, et al. (2020) Optimization of casting means and heat treatment routines for improving mechanical and corrosion resistance properties of A356–0.54Sc casting alloy. *Mater Today Commun* 24: 101227. https://doi.org/10.1016/j.mtcomm.2020.101227

AIMS Press